# Nanoscale

Accepted Manuscript


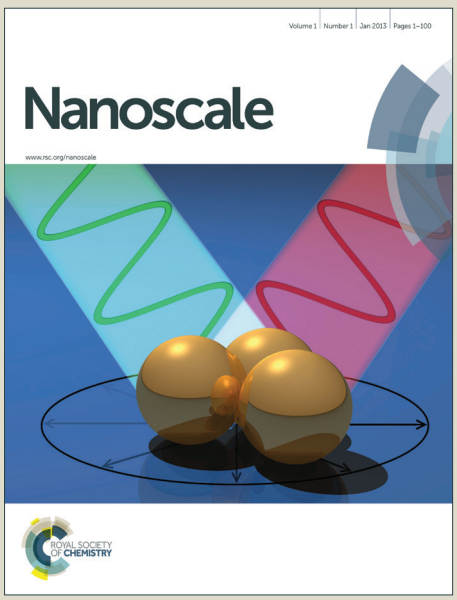





ROYAL SOCIETY OF CHEMISTRY

www.rsc.org/nanoscale

Nanoscale

RSCPublishing

ARTICLE

# Diameter-Selective Electron Transfer from Encapsulated Ferrocenes to Single-Walled Carbon Nanotubes

Cite this: DOI: 10.1039/x0xx00000x

Received 00th January 2012,
Accepted 00th January 2012

DOI: 10.1039/x0xx00000x

www.rsc.org/

Yoko Iizumi, [a] Hironori Suzuki, [b] Masayoshi Tange[a] and Toshiya Okazaki [a,b*]

The diameter-selective photoluminescence quenching of single-walled carbon nanotubes (SWCNTs) is observed upon ferrocene encapsulation, which can be attributed to electron transfer from the encapsulated ferrocenes to the SWCNTs. Interestingly, the dependence of the electron transfer process on the tube diameter is governed by the molecular orientation of the ferrocenes in the SWCNT rather than the reduction potentials of the SWCNT.



## Introduction

Single-walled carbon nanotubes (SWCNTs) have strong potential as electronic devices as a result of their high mobility, flexibility, and applicability in solution processing.[1] For device applications, carrier doping is one of the most important techniques for contracting complementary electronics. For instance, in complementary metal-oxide-semiconductor (CMOS)-type logic gates, both p-type and n-type transistors are used on the same integrated circuit.[2,3] Also, in other applications, such as photovoltaic cells[4] and thermo-piles,[5,6] the control of semiconducting properties is essential for fabricating the desired devices. However, semiconducting SWCNTs cannot be doped using the traditional approach for bulk semiconductors—ion implantation—because substituted dopants significantly destroy the CNT lattice, which introduces flaws in the inherent properties of the SWCNTs. For this reason, charge-transfer doping has commonly been employed.

In particular, the encapsulation of organic molecules and organometallic complexes into the interior spaces of SWCNTs has been successful for carrier doping in a controllable way.[7,8] Doping molecules into the inner spaces instead of the exteriors of the SWCNTs is expected to be a useful technique for achieving realistic applications of SWCNTs by increasing their stability and durability. The carrier density can be controlled by the ionization potential ($I_p$) and the electron affinity ($E_a$) of the encapsulated materials.[7] It was reported that molecules having $I_p$ < ~6.5 eV can supply their electrons to SWCNTs with diameters ($d_t$) of ~1.4 nm.[7] On the other hand, molecules having $E_a$ > ~2.7 eV accept electrons from the SWCNTs.[7]
The organometallic compound, ferrocene ($FeCp_2$), is frequently used as encapsulated molecules.[9–15] Because of its lower $I_p$ (= 5.88 eV),[16] electron transfer from the encapsulated $FeCp_2$ to SWCNTs can be expected.[7] Indeed, photoemission studies unveiled the electron doping process that took place from $FeCp_2$ to SWCNTs, which was rationalized by density functional theoretical calculations.[12,13] The number of transferred electrons was estimated to be 0.14 per $FeCp_2$.[13] However, the observed phenomena were average behaviors of various SWCNTs having many ($n$, $m$) species, and information with respect to the responses of individual ($n$, $m$) tubes has so far been limited.

Recently, a photoluminescence (PL) study of $FeCp_2$-encapsulated SWCNTs ($FeCp_2$@SWCNTs) was reported.[15] Generally, the PL method can provide rich information about the electronic properties of individual ($n$, $m$) nanotubes at a resolution of a few meV.[17] Upon $FeCp_2$ encapsulation, increases in the PL intensities were observed for some SWCNTs.[15] This behavior was attributed to local electron transfer from encapsulated $FeCp_2$ molecules to SWCNTs that were p-doped during the end-opening process and surfactant molecules.

One of the important factors for the observed PL behavior was the diameter of the SWCNTs, because the alignment of the $FeCp_2$ molecules was expected to change depending on the tube

diameter.[12,14,15,18] To further characterize the $FeCp_2$ encapsulation effect, $FeCp_2$@SWCNTs with varying diameters require investigation. In a previous report, SWCNTs produced by the HiPco method were used as templates of $FeCp_2$@SWCNTs.[15] The diameters of the examined HiPco-SWCNTs ranged from 0.75 nm to 1.1 nm.[15]

We here report the PL spectroscopic characterization of $FeCp_2$@SWCNTs with diameters ranging from 0.8 to 1.4 nm. A further investigation over a wide range of $d_t$ clearly uncovered the diameter-dependent electron transfer between $FeCp_2$ and SWCNTs, and the importance of the molecular orientation of $FeCp_2$ in the SWCNTs.

## Results and discussion

Figure 1 (a-d) show typical high-resolution transmission electron microscope (HRTEM) images of $FeCp_2$@SWCNTs. HRTEM measurements were performed with a JEM-2100F at an accelerating voltage of 120 kV. The image exhibited dark contrasts distributed inside the SWCNT. The image simulation (Fig. 1(e)), calculated using the structure model (Fig. 1(f)), showed that $FeCp_2$ molecules were certainly encapsulated in the SWCNTs (Fig. 1(d)). It is noted that the arrangements of the $FeCp_2$ molecules inside SWCNTs were substantially affected by the electron beam irradiations.[19] Therefore, the observed images do not exhibit the stable structures under the ambient condition.

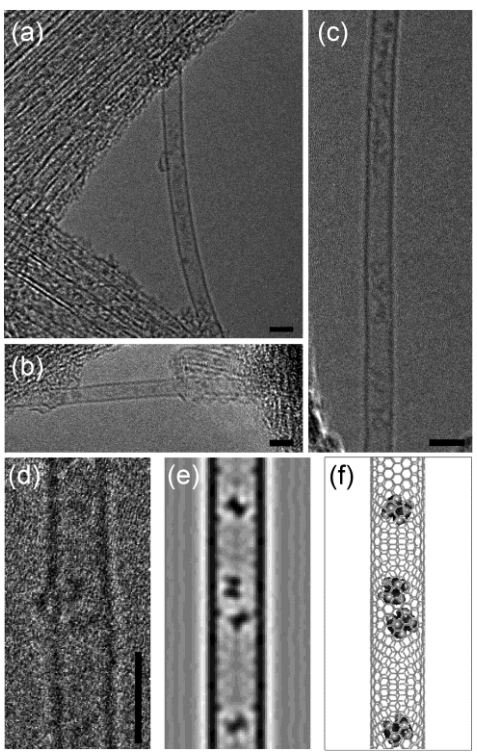


**Fig. 1** (a-d) Typical HRTEM images of $FeCp_2$@SWCNTs (scale bars = 2 nm). (e) The simulated image of Figure 1(d) and (f) the corresponding molecular structure.

Figure 2 shows the PL intensity contour maps of (a) a SWCNTs control sample and (b) $FeCp_2$@SWCNTs as a function of emission ($\lambda_{11}$) and excitation ($\lambda_{22}$) wavelengths. The PL peaks on the maps are clearly seen in the second interband ($E_{22}$) excitation region ($\lambda_{22}$ = 550–950 nm) and the first interband ($E_{11}$) emission region ($\lambda_{11}$ = 1000–1750 nm) of SWCNTs with diameters of 0.8–1.4 nm, which can be assigned to specific (*n*, *m*) SWCNTs by the empirical relationships of Weisman *et al*.[20]

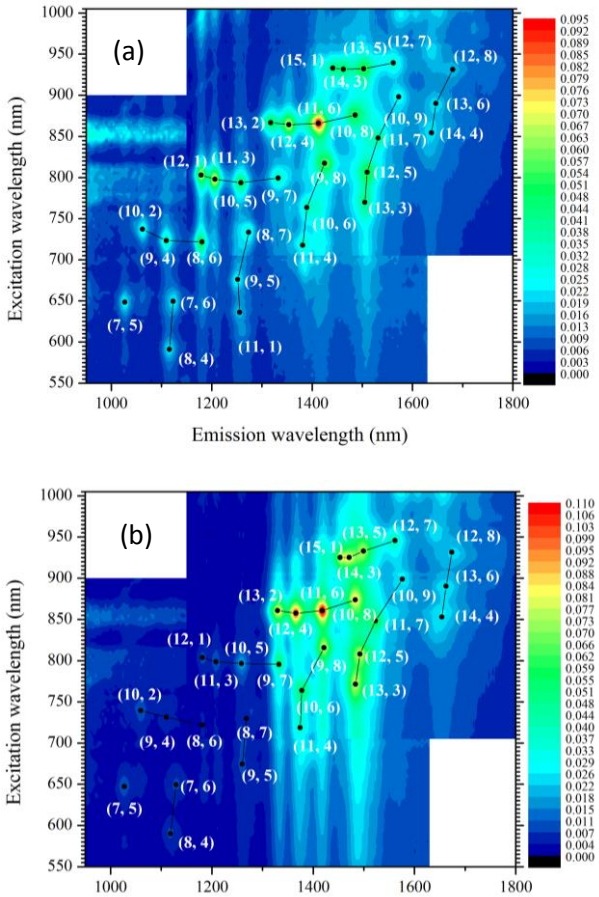


**Fig. 2** Near-infrared photoluminescence maps of (a) SWCNTs and (b) $FeCp_2$@SWCNTs in sodium dodecylbenzenesulfonate (SDBS)-$D_2O$. The same "2*n* + *m*" values are connected.

Although the PL pattern of $FeCp_2$@SWCNTs showed a characteristic "2*n* + *m*" family pattern (Fig. 2(b)),[16,20] the PL intensities at around $\lambda_{11}$ = 1200 nm were strongly quenched as compared to the SWCNTs control sample (Fig. 2(a)). For example, the PL peaks of (8, 6), (8, 7), and (12, 1) became very weak in the PL map of $FeCp_2$@SWCNTs, whereas they were clearly observed in that of the SWCNTs control sample (Fig. 2(a)).

To elucidate the difference in the PL intensities between the $FeCp_2$@SWCNTs and the SWCNTs control sample, we plotted the PL intensity ratio of $FeCp_2$@SWCNTs and SWCNTs ($I_{PL}^{FeCp2@SWCNTs}/I_{PL}^{SWCNTs}$) as a function of the tube diameter (Fig. 3). Apparently, $I_{PL}^{FeCp2@SWCNTs}/I_{PL}^{SWCNTs}$ can be classified

into three regions depending on the diameter. Starting from smaller $d_t$, the values of $I_{PL}^{FeCp2@SWCNTs}/I_{PL}^{SWCNTs}$ decreased stepwise at $d_t$ ~ 0.92 nm, as indicated by the dotted line in Fig. 3. It is worth noting that theoretical calculations and experimental observations predicted that $d_t$ ~0.9 nm is the smallest $d_t$ for encasing the $FeCp_2$ molecules,[14,15] which exactly matched the threshold value for the PL reduction deduced from Fig. 3. This agreement strongly suggested that the encapsulation of $FeCp_2$ in SWCNTs resulted in the quenching of PL emissions. As $d_t$ increased, the PL emissions became brighter again at $d_t$ > 1.07 nm (the second dotted line in Fig. 3).

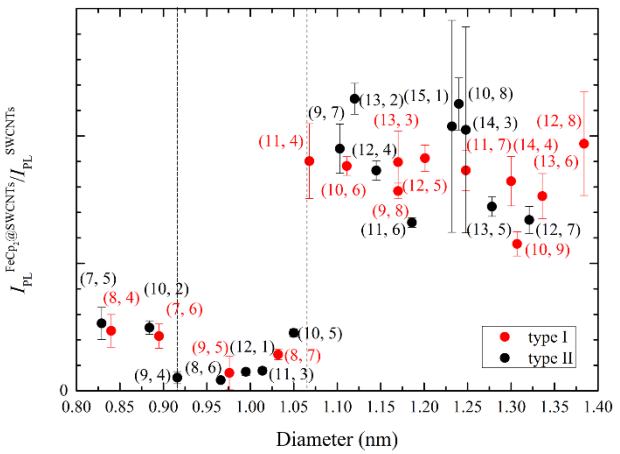


**Fig. 3** PL intensity ratio between $FeCp_2$@SWCNTs and SWCNTs ($I_{PL}^{FeCp2@SWCNTs}/I_{PL}^{SWCNTs}$) as a function of tube diameter. The SWCNTs shown here are classified by the so-called "2*n*+*m*" family types (type I (mod(2*n*+*m*, 3) = 1) and type II (mod(2*n*+*m*, 3) = 2)).

Meanwhile, the optimized molecular arrangements of $FeCp_2$ in SWCNTs have been investigated by theoretical calculations (see Fig. S1).[12,14,15,18] For smaller diameter tubes (0.94 nm < $d_t$ < 1.02 nm), $FeCp_2$ was fully aligned with an orientation parallel to the tube axis.[14] At $d_t$ = 1.17 nm, $FeCp_2$ began to oscillate and adopt an orientation with its molecular axis oriented perpendicularly to the tube axis.[14] The molecular orientation of the encapsulated $FeCp_2$ should affect the electron transfer from $FeCp_2$ to SWCNTs. Mulliken-population analysis was conducted for the (8, 6), (9, 5), and (16, 0) tubes with diameters of 0.966 nm, 0.976 nm, and 1.270 nm, respectively.[15] The encapsulated $FeCp_2$ molecules adopted parallel and perpendicular alignments for the former two and the latter tubes, respectively. The extent of electron transfer was found to be larger in the former cases than the last case.[15]

These theoretical results implied that the selective quenching of the PL intensity for 0.92 nm < $d_t$ < 1.05 nm could be attributed to electron transfer from $FeCp_2$ that was aligned in a parallel fashion to the outer SWCNTs, because carrier doping usually diminishes the PL intensity of SWCNTs.[21,22] If the tube diameter was greater than ~1.07 nm, $FeCp_2$ molecules could find enough space to "stand up" inside the SWCNTs; the electron transfer does not proceed very much in that configuration. As a result, the PL signals were observable again. The previous PL study reported that the electron transfer from the $FeCp_2$ to the SWCNTs occurred in almost the same diameter region (~0.9 nm < $d_t$ < ~1.05 nm), but led to PL enhancements.[15] One possible reason for the different PL behaviors might be due to the doping level of the original SWCNTs. In the case of the previous study, the SWCNTs were considered to be p-doped by the end-opening and solvation processes.[15] On the other hand, the SWCNTs used here were annealed to remove impurities under vacuum after the purification and the end-opening processes, which may have weakened the doping effects in the original SWCNTs (see Fig. S2).

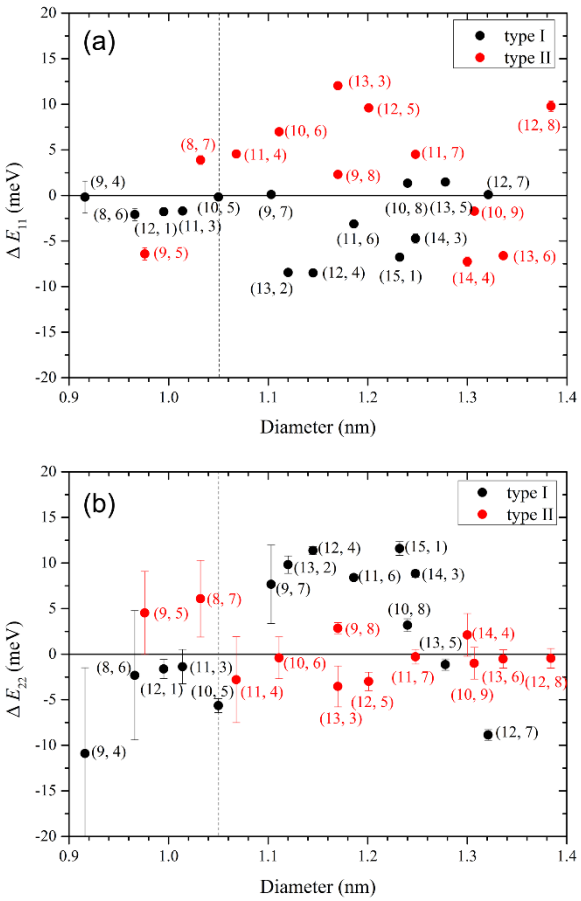


**Fig. 4** PL intensity ratio between $FeCp_2$@SWCNTs and SWCNTs ($I_{PL}^{FeCp2@SWCNTs}/I_{PL}^{SWCNTs}$) as a function of tube diameter.

Besides the intensity changes, shifts in the PL peak positions were also observed upon $FeCp_2$ encapsulation (Fig. 2 and Fig. S3 in Supporting Information). Figure 4 shows the $FeCp_2$ encapsulation effect on the optical transition energies in $E_{11}$ and $E_{22}$, in which the energy differences in $E_{11}$ and $E_{22}$ between $FeCp_2$@SWCNTs and SWCNTs ($\Delta E_{ii} = E_{ii}^{FeCp2@SWCNTs} - E_{ii}^{SWCNTs}$, $i$ = 1, 2) are plotted as a function of tube diameter ($d_t$

> 0.92 nm). Clearly, the dependence on diameter of $\Delta E_{11}$ and $\Delta E_{22}$ was different between type I (mod($2n + m$, 3) = 1) and type II (mod($2n + m$, 3) = 2) tubes. The $\Delta E_{11}$ for type I tubes exhibited a concave-shaped diameter dependence with a maximum at $d_t$ ~ 1.2 nm (Fig. 4(a)). On the contrary, a convex shape could be observed with a minimum at $d_t$ ~ 1.2 nm for the type II tubes. As was the case with $\Delta E_{11}$, $\Delta E_{22}$ also showed clear tube type dependence (Figure 4(b)). Namely, $\Delta E_{22}$ for type I tubes showed a maximum at $d_t$ ~1.2 nm, whereas $\Delta E_{22}$ for type II tubes exhibited the opposite diameter dependence (Figure 4(b)). Clear energetic shifts in $E_{11}$ and $E_{22}$ at $d_t$ > 1.07 nm indicated that the $FeCp_2$ molecules were reliably encapsulated for these tubes, but still showed PL signals (Fig. 2(b)).

In the case of $C_{60}$ encapsulated in SWCNTs (nanopeapods), similar tube-type and diameter dependences in $\Delta E_{11}$ and $\Delta E_{22}$ were observed.[23-26] The effects of $C_{60}$ on the optical transition energies of SWCNTs can be explained by a weak intermolecular interaction.[23–26] The PL and resonance Raman results suggested that the smallest $d_t$ for encapsulating $C_{60}$ without friction was ~1.32 nm, and the interaction due to the attractive intermolecular force was most effective at ~1.4 nm.[23–26] Analogous to $C_{60}$ nanopeapods, it was expected that the interaction between perpendicularly aligned $FeCp_2$ and SWCNTs would become most attractive at around ~1.15 (= 1.07 + 0.08) nm. In fact, the diameter dependence of $\Delta E_{11}$ and $\Delta E_{22}$ observed here suggested that the interaction between $FeCp_2$ and the SWCNTs reached a maximum at ~1.2 nm (Fig. 4). The coincidence of the critical diameters strongly suggested that the interaction between $FeCp_2$ and SWCNTs would be dominated by the intermolecular interaction for $d_t$ > 1.07 nm.

The present findings unveiled that electron transfer from the encapsulated $FeCp_2$ to the SWCNTs was not determined by the reduction potential of the SWCNTs. Electrofluorescence measurements indicated that, as $d_t$ increased, the reduction potential of the SWCNTs slightly decreased.[22] The lower reduction potential is more favorable for accepting electrons. However, in the $FeCp_2$@SWCNTs, the electron transfer occurred only in the smaller diameter tubes (0.92 nm < $d_t$ < 1.05 nm), even though they have larger reduction potentials.[22] This finding provides a deep insight into the carrier doping of SWCNT-based materials. Not only the $I_p$ and $E_a$ of the dopant, but also deeper considerations, such as the orientation of the dopant, are important for obtaining the desired properties.

## Experimental

### Synthesis of ferrocene-encapsulated SWCNTs ($FeCp_2$@SWCNTs).

The encapsulation of ferrocene ($FeCp_2$) (Tokyo Chemicals Industry) inside SWCNTs was achieved through vapor phase doping. Briefly, SWCNTs (KH Chemicals, ED grade) were purified by the protocol described in the literature.[24] The purified SWCNTs were heated at 500°C for 30 min to open the caps of the SWCNTs, and sealed with $FeCp_2$ in a quartz tube under vacuum (~$1 \times 10^{-4}$ Pa). On heating at 200–300°C, $FeCp_2$ molecules sublimed individually and migrated into the SWCNTs (~24 h). The synthesized $FeCp_2$@SWCNTs were washed with toluene and annealed at ~300°C under vacuum conditions to remove excess $FeCp_2$ adhering to external surfaces.

Aqueous micellar solutions of $FeCp_2$@SWCNTs for absorption, fluorescence, excitation, and PL measurements were prepared in a similar way to the procedure described by Bachilo et al.[17] Typically, $FeCp_2$@SWCNTs (~1 mg) were dispersed for 10 min in $D_2O$ (~20 mL) containing 1 wt% sodium dodecylbenzenesulfonate (SDBS) (WAKO Chemicals) using a 200 W homogenizer (SONICS VCX500) equipped with a titanium alloy tip (TI-6AL-4V). Each solution was then centrifuged at 123000 g for 2.5 h (HITACHI CP 100MX) and the supernatant was used in further studies.

### Photoluminescence spectroscopy.

Photoluminescence (PL) spectroscopy was conducted with Horiba JY Fluorolog 3-2 TRIAX and Shimadzu NIR-PL systems. We used the latter system for the regions $\lambda_{11}$ = 1150–1800 nm and $\lambda_{22}$ = 700–1000 nm. The spectral regions $\lambda_{11}$ = 950–1630 nm and $\lambda_{22}$ = 550–900 nm were measured with the Fluorolog system. To combine the PL maps obtained by the NIR-PL and Fluorolog systems, we normalized the peak intensities of the (11, 6) tubes (Fig. 2).

## Conclusion

The effect of $FeCp_2$ encapsulation on the SWCNTs electronic state was investigated using PL spectroscopy over a wide tube diameter range ($d_t$ = 0.8–1.4 nm). The present results suggest that the interaction between $FeCp_2$ and the SWCNTs is dependent on the tube diameter. In the smaller diameter range of 0.96–1.06 nm, electron transfer occurred from $FeCp_2$ to the SWCNTs, which resulted in PL quenching. With increasing $d_t$, the interaction changed to intermolecular interactions committed among both at diameters of 1.06–1.35 nm. Importantly, the electron transfer process in $FeCp_2$@SWCNTs was not dominated by the reduction potential of the SWCNTs, but by the molecular orientation of the encapsulated $FeCp_2$. This would undoubtedly be an important advance in development of SWCNT-based electronics and sensory applications.

## Acknowledgements

The authors thank K. Sakai (TASC/AIST) for experimental assistance. We also thank Professor L. Bolotov (University of Tsukuba) for his kind advice. This work was partly supported by a Grant-in-Aid for Young Scientists (A) (#21685017).

## Notes and references



 

[a] Nanotube Research Center, National Institute of Advanced Industrial Science and Technology (AIST), Tsukuba 305-8565, Japan.
E-mail: toshi.okazaki@aist.go.jp
[b] Department of Chemistry, University of Tsukuba, Tsukuba 305-8577, Japan.

† Electronic Supplementary Information (ESI) available: [Calculated binding energies of FeCp2@SWCNTs and additional spectroscopic characterization are described in ESI.]. See DOI: 10.1039/b000000x/

1 Ph. Avouris and J. Chen, *Mater. Today*, 2006, **9**, 46.
2 V. Derycke, R. Martel, J. Appenzeller and Ph. Avouris, *Nano Lett.*,. 2001, **1**, 453.
3 A. Bachtold, P. Hadley, T. Nakanishi and C. Dekker, *Science*, 2001, **294**, 1317.
4 L. Yang, S. Wang, Q. Zeng, Z. Zhang, T. Pei, Y. Li and L.-M. Peng, *Nat. Photonics*, 2011, **5**, 672.
5 C. Hu, C. Liu, L. Chen, C. Meng and S. Fan. *ACS Nano*, 2010, **4**, 4701.
6 B. C. St.-Antoie, D. Ménard and R. Martel, *Nano Lett.*, 2011, **11**, 609.
7 T. Takenobu, T. Takano, M. Shiraishi, Y. Murakami, M. Ata, H. Kataura, Y. Achiba and Y. Iwasa, *Nat. Mater.*, 2003, **2**, 683.
8 L.-J. Li, A. N. Khlobystov, J. G. Wiltshire, G. A. D. Briggs and R. J. Nicholas, *Nat. Mater.*, 2005, **4**, 481.
9 L. Guan, Z. Shi, M. Li and Z. Gu, *Carbon*, 2005, **43**, 2780.
10 Y. Li, R. Hatakeyama, T. Kaneko and T. Okada, *Jpn. J. Appl. Phys.*, 2006, **45**, L428.
11 Y. F. Li, R. Hatakeyama, T. Kaneko, T. Izumida, T. Okada and T. Kato, *Appl. Phys. Lett.*, 2006, **89**, 083117.
12 H. Shiozawa, T. Pichler, C. Kramberger, A. Grüneis, M. Knupfer, B. Büchner, Z. Zólyomi, J. Koltai, J. Kürti, D. Batchelor and H. Kataura, *Phys. Rev. B*, 2008, **77**, 153402.
13 H. Shiozawa, T. Pichler, A. Grüneis, R. Pfeiffer, H. Kuzmany, Z. Liu, K. Suenaga and H. Kataura, *Adv. Mater.*, 2008, **20**, 1443.
14 W. Plank, R. Pfeiffer, C. Schaman, H. Kuzmany, M. Calvaresi, F. Zerbetto and J. Meyer, *ACS Nano*, 2010, **4**, 4515.
15 X. Liu, H. Kuzmany, P. Ayala, M. Calvaresi, F. Zerbetto and T. Pichler, *Adv. Funct. Mater.*, 2012, **22**, 3202.
16 C. Cauletti, J. C. Green and M. R. Kelly, *J. Electron Spectrosc. Relat. Phenom.*, 1980, **19**, 327.
17 S. M. Bachilo, M. S. Strano, C. Kittrell, R. H. Hauge, R. E. Smalley and R. B. Weisman, *Science*, 2002, **298**, 2361.
18 E. L. Sceats and J. C. Green, *J. Chem. Phys.*, 2006, **125**, 154704.
19 T. Okazaki, K. Suenaga, K. Hirahara, S. Bandow, S. Iijima and H. Shinohara, *J. Am. Chem. Soc.*, 2001, **123**, 9673.
20 R. B. Weisman and S. M. Bachilo, *Nano Lett.*, 2003, **3**, 1235.
21 M. J. O'Connell, E. E. Eibergen and S. K. Doorn, *Nat. Mater.*, 2005, **4**, 412.
22 Y. Tanaka, Y. Hirana, Y. Niidome, K. Kato, S. Saito and N. Nakashima, *Angew. Chem. Int. Ed.*, 2009, **48**, 7655.
23 T. Okazaki, S. Okubo, T. Nakanishi, S.-K. Joung, T. Saito, M. Otani, S. Okada, S. Bandow and S. Iijima, *J. Am. Chem. Soc.*, 2008, **130**, 4122.
24 S. Okubo, T. Okazaki, N. Kishi, S.-K. Joung, T. Nakanishi, S. Okada and S. Iijima, *J. Phys. Chem. C*, 2009, **113**, 571.
25 S.-K. Joung, T. Okazaki, N. Kishi, S. Okada, S. Bandow and S. Iijima, *Phys. Rev. Lett.*, 2009, **103**, 027403.
26 S.-K. Joung, T. Okazaki, S. Okada and S. Iijima, *J. Phys. Chem. C*, 2012, **116**, 23844.

**TOC graphics**

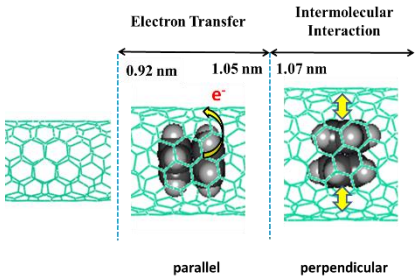


The diameter-selective photoluminescence quenching of single-walled carbon nanotubes (SWCNTs) is observed upon ferrocene encapsulation, which can be attributed to electron transfer from the encapsulated ferrocenes to the SWCNTs.